8-Hydroxyquinoline Monomer, Water Adducts, and Dimer. Environmental Influences on Structure, Spectroscopic Properties, and Relative Stability of *Cis* and *Trans* Conformers

Mario Amati, Sandra Belviso, Pier Luigi Cristinziano, Camilla Minichino, and Francesco Lelj*

La. MI Dipartimento di Chimica and LaSCAMM, CR-INSTM Unità della Basilicata Università della Basilicata, Via Nazario Sauro 85, 85100 Potenza, Italy

Iolinda Aiello, Massimo La Deda, and Mauro Ghedini*

Centro di Eccellenza CEMIF. CAL-LASCAMM, CR-INSTM Unità della Calabria, Dipartimento di Chimica, Università della Calabria, I-87036 Arcavacata di Rende (CS), Italy

Received: June 11, 2007; In Final Form: October 15, 2007

The low fluorescence quantum yield of 8-hydroxyquinoline cannot be correctly interpreted without knowing the form that such a compound assumes in different environments. The commonly accepted emission-quenching excited-state proton transfer can follow different reaction paths if 8-hydroxyquinoline is dimeric or monomeric or if it exists in the form of *cis* and *trans* conformers; in this light, the knowledge of the compound form in a particular environment is basic. We have performed a spectroscopic and computational investigation aimed at the determination of the form of 8-hydroxyquinoline in different solvents. UV−vis, fluorescence, and IR spectral features have been assigned by *ab initio* computations based on the density functional theory and time-dependent density functional theory; the density functional theory and MP2 computations have been applied to the determination of the relative stability of the dimeric and monomeric *cis* and *trans* forms of 8-hydroxyquinoline in different solvents. Molecular dynamics computations have been used to determine the compound behavior in water solutions. According to our results, 8-hydroxyquinoline shows a clear preference for the *cis* conformation (as dimer or monomer), but, in water solutions, a small fraction of the *trans* conformation is also present.

Introduction

8-Hydroxyquinoline is a known complexating agent. It is also known as oxine, especially in analytical chemistry, but we will refer to it as 8HQ in the following. The 8HQ structure is shown in Figure 1; 8HQ can assume two isomeric forms that will be referred to as *cis*-8HQ and *trans*-8HQ in the following. When its phenolic-like OH function is deprotoned, the resulting anion quinolin-8-olate ($8Q^-$) acts as a bidentate ligand that is able to bind metal cations so effectively that its chelating ability is considered only second to EDTA.[1] Although this finding is already sufficient for fruitful application of such a molecule, 8HQ has been extensively used for the fluorogenic determination of metal cations,[2] also taking advantages from its chelating ability as a means to concentrate metals before the fluorometric determination.[3] In fact, 8Q coordination compounds are often strongly emissive both in solution and in solid phases; this feature is exploited in the use of such complexes as emissive materials in the emerging display technology based on organic light emitting diodes (OLEDs).[4]

Although $8Q^-$ forms very fluorescent metal complexes, 8HQ is weakly emissive. According to Ballard and Edwards,[5] the observed 8HQ low fluorescence quantum yield in many solvents and in wide ranges of solvent acidity has to be assigned to a tautomerization process that takes place in the excited state. The process consists of a proton transfer from the OH function to the N function of 8HQ, and it is referred to as excited-state proton transfer (ESPT). The resulting ketonic form of 8HQ is supposed to be barely emissive. The authors observed that, in H_2O solution, excited-state protonation of the N function of 8-methoxyquinoline (8MeQ) is too slow to take place before deactivation to the ground state. By virtue of the great similarity between geometrical and electronic properties of 8MeQ and 8HQ, they concluded that, if the ESPT quenches fluorescence, it has to be an intramolecular process and/or the presence of the OH proton should be decisive.

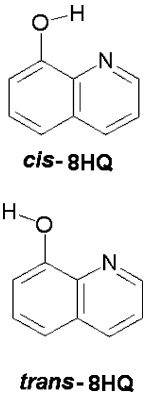

Figure 1. *cis*-8HQ and *trans*-8HQ isomers of 8-hydroxyquinoline.

Goldman and Wehry[6] studied solvation and temperature influences on the fluorescence quantum yields of 8HQ and 5-hydroxyquinoline (5HQ). 5HQ is similar to 8HQ, but it is unable to form the intramolecular hydrogen bond. The authors noted that 5HQ fluorescence quantum yield decreases in solvents

* Corresponding author. E-mail: francesco.lelj@unibas.it. Fax: +39(0)971202223. Tel. +39(0)971202246.

10.1021/jp074510s CCC: $37.00
Published on Web 12/06/2007

capable of forming strong hydrogen bonds with the OH function. The clear correlation between the ability of forming hydrogen bonds and the fluorescence quantum yield led the authors to conclude that the presence of the intramolecular hydrogen bond in 8HQ is the principal cause of the poor fluorescence of the molecule. The fact that 8HQ is poorly emissive in alkane and H_2O, but relatively emissive in solvents like THF and chloroform was explained with the limited ability of these solvents to form fluorescence-quenching hydrogen bonds with 8HQ and, at the same time, its sufficient ability to disrupt the intramolecular hydrogen bond. The thesis of the ESPT as quencher of emission was further defended by Shulman[7] and appears to be the most considered theory in the late sixties and starting seventies.[8]

Recent investigations have pointed out a further complication. According to osmometry measures of Bardez et al.,[9] different solvents have strong influences on the aggregation behavior of 8HQ. In *n*-heptane solution, 8HQ appears to form strong dimers. According to the authors, it is likely that this is the form of 8HQ also in other alkane solutions by virtue of the observed similarity of the IR and UV−vis spectra in *n*-heptane and cyclohexane solutions. Furthermore, the narrowness of the OH stretching band in these solvents suggests the presence of well defined and kinetically stable dimers on the IR time scale. In chloroform solutions, osmometry measures indicated that 8HQ, in the concentration range from 1.3×10^{-2} to 5.14×10^{-2} M, forms 1:1 adducts with one H_2O molecule. Also in this case, the authors suggest that this is the form of 8HQ in other chlorinated solvents like CH_2Cl_2 on the basis of indirect observations.

The importance of the study of Bardez et al.[9] is the recognition that a detailed explanation of 8HQ fluorescence quenching should be strictly related to the particular form that 8HQ assumes in a specific environment. If the ESPT is so fast to occur in the excited state, it should follow different reaction paths in alkane solutions and chlorinated (or H_2O) solutions. The dimeric form of 8HQ in alkane solutions has been suggested to parallel 8HQ with 7-azaindole.[10] 7-Azaindole is a sort of a prototype compound for the double proton transfer when it is prepared in dimeric form in alkane solutions. This fact, together with the structural similarity between the two compounds, suggested that an excited-state double proton transfer also takes place in 8HQ dimers.[10]

The issue of structure and behavior of H_2O−8HQ adducts is a not simple task. Li and Fang[11] have performed *ab-initio* computations on one possible 1:1 H_2O−8HQ adduct. According to their work, the presence of one H_2O molecule interposed between the OH and N functions in *cis*-8HQ lowers the energy barrier of the proton transfer in the first excited state. Furthermore, a concerted proton transfer involving 8HQ and H_2O is modeled as a single-barrier path. However, the authors have only reported a detailed study of three stationary points of the potential energy surface (PES) of one of the 1:1 *cis*-8HQ−H_2O adduct. They have not investigated the possibility that H_2O molecules can induce *cis*−*trans* isomerization in the ground state, with a consequent drastic change in the ESPT reaction path. Furthermore, they have only investigated one of the possible adducts involving *cis*-8HQ and H_2O, whereas several minima points of the PES are reasonably predicted for several relative dispositions of H_2O and 8HQ.

trans-8HQ cannot form the intramolecular hydrogen bond; thus, the intramolecular ESPT cannot take place in this conformer. In solvents like H_2O, the hydrogen bond ability of solvent molecules could favor the *trans*-8HQ isomer. It is possible that the presence of 1:1 H_2O−8HQ adducts in chlorinated solvents could lead to a fraction of 8HQ as *trans*-8HQ. This could explain the relatively intense fluorescence in solvents like $CHCl_3$, CH_2Cl_2, and THF; in fact, the intramolecular ESPT cannot take place in *trans*-8HQ and the solvent cannot operate as acid or base in the intermolecular ESPT. On the other hand, the postulated 8HQ intramolecular hydrogen bond could not exist in H_2O or in H_2O-containing solvents even though the molecule exists as *cis* conformer. A H_2O molecule could be invariably interposed in the intramolecular hydrogen bond, and its influence on the ESPT could be always present. The high reaction rate of tautomerization allows us to discard the hypothesis of *cis*-*trans* isomerization during the proton transfer.

Thus, it appears of great importance to clarify the preferred form of 8HQ in different solvents and the possible influence of solvent−8HQ hydrogen bonds on the relative stability of the *cis* and *trans* isomers. This is the basic knowledge for any hypothesis about the emission quenching mechanism. In fact, different forms of 8HQ (dimeric 8HQ, 1:1 H_2O−8HQ adducts in *cis* or *trans* conformations) have to be associated to quenching reaction paths that are different in principle.

In this paper, we try to shed light on the form assumed by 8HQ in different solvents with the aim to support future investigations about the detailed fluorescence quenching mechanism. We have combined UV−vis and vibrational spectroscopic observations with quantum-chemical *ab-initio* and classic molecular dynamics computations with the aim to understand the *cis*−*trans* conformational equilibrium of 8HQ in alkane solutions, chlorinated solutions, and H_2O solutions. Direct interaction between 8HQ and H_2O has been taken into account in our computational work, so that we can report a quantitative estimate of the relative stability of the *cis* and *trans* isomers with and without the presence of hydrogen bonds with solvent molecules. Influences of hydrogen bonds on the UV−vis and vibrational absorptions have been investigated.

Methods

Experimental Methods. 8-Hydroxyquinoline and KBr were obtained from Aldrich and used without any purification. Spectrofluorometric grade solvents (Acros Organics) were used for the photophysical investigations in solution at room temperature. A Perkin-Elmer Lambda 900 spectrophotometer was employed to obtain the UV−vis absorption spectra, and the corrected emission spectra, all confirmed by excitation ones, were recorded with a Jobin Yvon Horiba Fluorolog-3 spectrofluorometer, equipped with Hamamatsu R928 photomultiplier tube. Emission quantum yields were determined using the optically dilute method on aerated solutions whose absorbance at excitation wavelengths was <0.1; $Ru(bpy)_3Cl_2$ (bpy = 2,2′-bipyridine) in H_2O was used as standard ($\Phi = 0.028$).[12,13] The experimental uncertainty on the emission quantum yields is 10%.

The room temperature infrared absorption spectra were recorded in the range 400−4000 cm^{-1} at a resolution of ±4 cm^{-1} using a single beam JASCO 460 Plus FT-IR spectrophotometer. Solution spectra were obtained using a 0.1 mm path length NaCl cell whereas the concentration of the solutions was tipically of 10^{-2} M.

Ab Initio Methods. Molecular geometries were optimized by using the Kohn−Sham density functional theory (DFT) with the 6-311G(2d,p) basis sets and the Becke three-parameters hybrid exchange-correlation functional known as B3LYP.[14] In some circumstances, smaller basis sets have been used for a rougher investigation of the potential energy surface. In this

case, the obtained minima were refined by using the larger base. The analytical evaluation of the energy second derivative matrix with respect to Cartesian coordinates (Hessian matrix) has always followed the geometry optimization and has been performed at the same level of approximation to confirm the nature of the stationary points associated to the optimized structures.

The post Hartree−Fock Møller−Plesset correlation method, truncated at the second-order (MP2),[15] has been used with the 6-311G(2d,p) basis set for single point computations on the B3LYP/6-311G(2d,p) geometries (MP2/6-311G(2d,p)//B3LYP/6-311G(2d,p) computation). Energy changes lower than 0.2 kcal/mol have been found by comparing the fully optimized structures at the MP2/6-311G(2d,p) level of approximation with the single point MP2/6-311G(2d,p)//B3LYP/6-311G(2d,p) computations described above (this test has been performed on the *cis*-8HQ, *trans*-8HQ, *cis*-adduct-1, and *trans*-adduct-1 structures discussed in the following).

Solvation effects have been included by treating the solvent by the IEF-PCM method (integral equation formalism polarizable continuum model).[16] Single point energy computations have been performed on the B3LYP/6-311G(2d,p) optimized structures.

Time dependent density functional theory (TD-DFT)[17,18] allowed the computation of excitation energies, oscillator strengths, and excited-state composition in terms of monoelectronic excitations between occupied and virtual Kohn−Sham orbitals. TD-DFT calculations were performed by using the same B3LYP functional and the 6-311+G(2d,p) basis set on the B3LYP/6-311G(2d,p) optimized structures.

All the computations were performed by using the Gaussian03 suite of programs Revision B.05.[19]

The figures have been produced by the programs Molden3.7[20] and Molekel4.3.[21]

Molecular Dynamics Methods. Molecular dynamics (MD) simulations were carried out with the Amber program version 6.0.[22] The calculations were carried out in H_2O with periodic boundary box. A rectangular cell was used with 256 H_2O molecules described by the TIP3P[23] model. An initial configuration was taken with 8HQ in *cis* conformation and H_2O adapted from a box of 216 molecules described by the TIP4P model[23] coming from a Monte Carlo liquid simulation. The force field is based on the empirical potential energy function:

$$V_{\text{total}} = \sum_{\text{bonds}} K_r(r - r_{\text{eq}})^2 + \sum_{\text{angles}} K_\theta(\theta - \theta_{\text{eq}})^2 + \sum_{\text{dihedrals}} \frac{V_n}{2}[1 + \cos(n\phi + \gamma)] + \sum_{i<j}\left\{\left[\frac{A_{ij}}{R_{ij}^{12}} - \frac{B_{ij}}{R_{ij}^{6}}\right] + \frac{q_i q_j}{\epsilon R_{ij}}\right\} + \sum_{\text{h\_bonds}}\left\{\frac{C_{ij}}{R_{ij}^{12}} - \frac{D_{ij}}{R_{ij}^{10}}\right\}$$

The function parameters are those of the Amber94 standard data base[24] and TIP3P[23] for H_2O. All the charges were divided by a factor 1.2 for evaluating the 1−4 interaction. The 1−4 Van der Waals interaction was scaled by a factor 0.5. The 8HQ charges were computed by the Gaussian03 package rev.B.05[19] using the Merz−Singh−Kollman[25] method and the B3LYP/6-31+G(d) level of approximation. Geometry optimization was performed at the same level of approximation before computing the atomic charges.

All the MD calculations were performed within the NPT ensemble at the temperature of 300 K and pressure of 0.1 MPa. Temperature scaling was made with the Berendsen algorithm[26] by using separate scaling factor for solute and solvent. The PME method[27] was used for the Coulombic interaction. A cutoff of 8.0 Å was applied for the Van der Waals interaction. The SHAKE algorithm[28] was used to constraint all the hydrogen atoms at their equilibrium distance values within each molecule. No further constrains were imposed to other internal geometrical parameters. The MD simulation time step was 1 fs and the simulation was conducted for 6 ns. The first 3 ns were discarded from analysis and used as equilibration time. Data for analysis were collected for the last 3 ns. According to the analysis, the computed density was 0.944 ± 0.013 g/dm^3 and energy of the whole system was 1918 ± 11 kcal/mol.

Spectroscopic Results

We have recorded absorption spectra in *n*-hexane (*n*-C_6H_{14} in the following), THF, $CHCl_3$, and H_2O solutions and as solid phase in the form of KBr pellets. Table S1 (in the Supporting Information) collects our results, and Figure 2 shows a typical 8HQ solution spectrum and some details of the recorded spectra.

8HQ shows two principal absorption bands. The first one has been found in the range from 305 to 320 nm and appears broader. The second one is more intense and sharper and it is placed in the range from 237 to 247 nm.

In the cases of *n*-C_6H_{14} solutions and $CHCl_3$ solutions we have measured the sample absorbance in the concentration range from 10^{-4} to 10^{-7} M. In such a range, the Lambert−Beer law can be considered satisfied in both the solvents and the molar absorbivity at peak wavelengths has been determined by a linear fit and reported in Table S1 (in the Supporting Information). The interested reader is directed to the Supporting Information for more details about the linear fit. These solvents have been chosen by virtue of the experimental evidence of dimeric 8HQ in alkane solutions and 1:1 H_2O−8HQ adducts in $CHCl_3$.[9] In spite of this difference due to solvation effects, we have found small changes in both peak wavelength and molar absorbivity in the case of the first band; a blue shift of 6 nm has been found in $CHCl_3$, the band shape and widths are very similar. Differently from the first band, the second absorption band seems more dependent on the environment: passing from *n*-C_6H_{14} to the $CHCl_3$ one, its peak molar absorbivity is significantly reduced and it is 3 nm red-shifted relative to *n*-C_6H_{14} solutions.

THF solution (1.0×10^{-5} M) shows absorption spectra similar to the $CHCl_3$. It is red-shifted and somewhat weaker. However, the band shape is very similar to the *n*-C_6H_{14} and $CHCl_3$ solutions, whereas the shape and molar absorbivity of the second absorption band are closer to those of $CHCl_3$ solutions.

H_2O solutions (1.0×10^{-5} M) present a different shape of the first absorption band (Figure 2) in comparison to *n*-C_6H_6, THF, and $CHCl_3$ (which show a clear similarity). Its peak wavelength is blue-shifted in comparison to the other solvents and this fact suggests an ipsochoromic behavior of this spectral feature (Table S1). The second absorption band is blue-shifted in comparison to *n*-C_6H_6 solutions, THF, and $CHCl_3$; thus, for this band, there is not a monotone shift of the peak wavelength with solvent polarity.

From the above, we can say that there exists a sort of discontinuity in the absorption features moving from THF and $CHCl_3$ to H_2O. This trend is paralleled by the changes in fluorescence quantum yields. As reported in the literature[6,9] and confirmed in this paper (Table S1), the fluorescence quantum yield is very low in *n*-C_6H_{14} and H_2O and higher in solvents of intermediate polarity like THF and $CHCl_3$. Furthermore, the

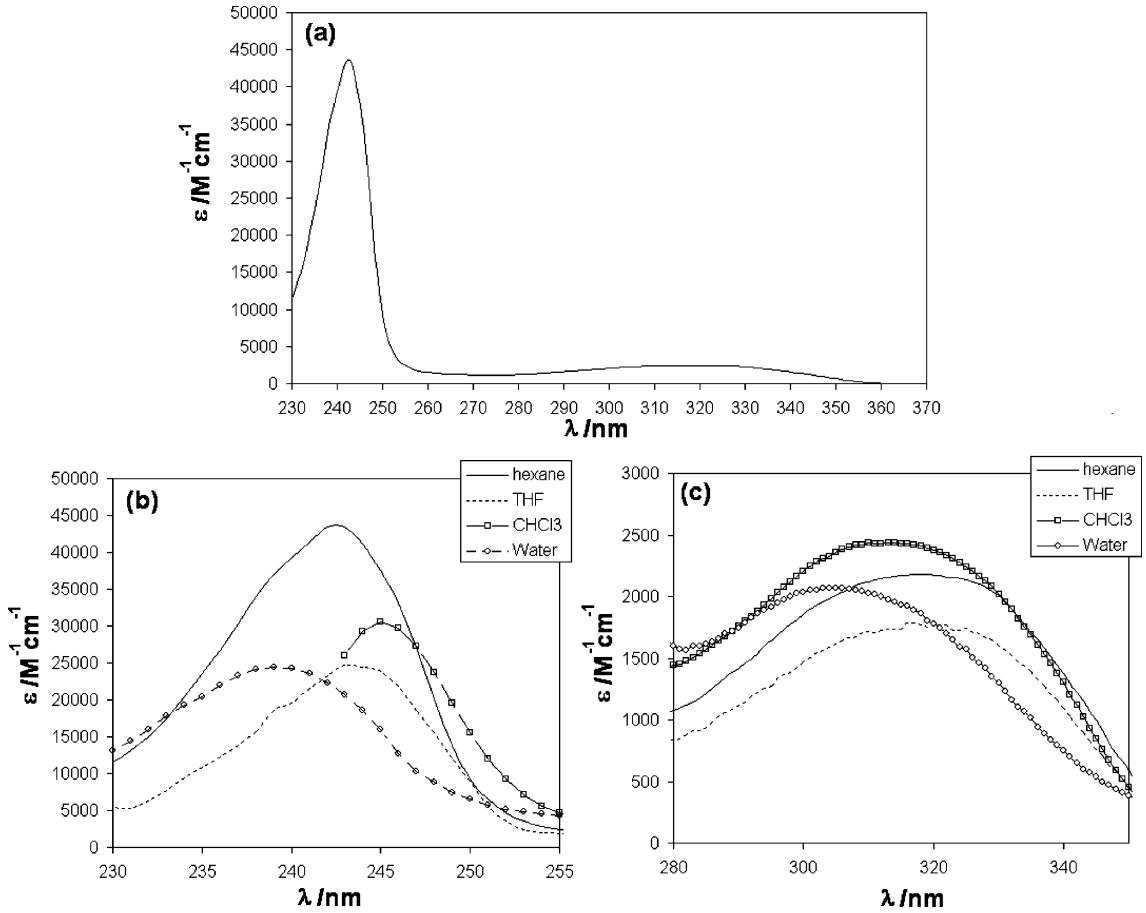

Figure 2. UV−vis spectra of 8HQ in different environments: (a) spectrum of 8HQ in *n*-C_6H_{14} solution (molar absorbivity versus wavelength); (b) more detailed plot of the 8HQ second absorption band and its variation with the environment; (c) more detailed plot of the 8HQ first absorption band and its variation with the environment.

TABLE 1: 8HQ OH Stretching Frequencies and Band Full Width at Half-Maximum (FWHM)

solvent	concentration (M)	stretching frequency (cm^{-1})	FWHM (cm^{-1})
n-C_6H_{14}	1.1×10^{-2}	3423	19
Et_2O	1.1×10^{-2}	3419	22
CCl_4	1.1×10^{-2}	3416	58
THF	1.0×10^{-2}	3406	65
$CHCl_3$	1.1×10^{-2}	3411	83

emission peak wavelength in H_2O is red-shifted by about 15 nm (Table S1). Such lacking of monotonic modification in the absorption and emission characteristics changing the solvent polarity can be traced to the different form of 8HQ in different solvents.

Solution IR spectra have been recorded with the aim to localize the OH stretching band in different solvents; such a band has been easily assigned according to previous works.[9,29] Table 1 lists some features of the recorded band. The most important point to be underlined is the substancial similarity in peak wavelength in environments that have heavy influences on the 8HQ form. Passing from dimeric 8HQ in apolar alkane to monomeric H_2O−8HQ adducts in $CHCl_3$ shifts the OH stretching frequency by 12 cm^{-1}; the peak wavelength spreads only 17 cm^{-1} in the set of used solvents. The negligible dependence of 8HQ OH stretching frequency has already been reported without a clear explanation.[30] It appears relatively easy to attribute this feature to the 8HQ intramolecular hydrogen bond, which is not affected by the environment and could be the primary reason for the OH force constant. However, the actual knowledge about 8HQ forms in different solvents allows us to formulate an alternative hypothesis. In the set of studied solvents, 8HQ could always exist as part of an adduct. It is aggregated to H_2O (like in $CHCl_3$ solutions) or to another 8HQ molecule (like in alkane solutions). In these 8HQ dimers, the reported high association constant[9] suggests a strong perturbation of the 8HQ OH force constant due to the strong intermolecular hydrogen bonds. Thus, the similarity in OH stretching frequency in the case of *n*-C_6H_6 and $CHCl_3$ solutions implies a similarly strong perturbation on the 8HQ OH force constant also in the case of H_2O−8HQ adducts. In other words, we suggest that 8HQ is normally aggregated to a second molecule by means of hydrogen bonds that have a similar effect on the 8HQ OH stretching frequency. We will return on the low variability of the OH stretching frequency in the following, when computational results will be reported.

Also if the similarity between 8HQ stretching frequencies in different solvents is clear and somewhat surprising, some environmental effects can be discussed. Like in UV−vis spectra and fluorescence emission quantum yields, a larger similarity in OH stretching wavenumber and bandwidth (FWHM) has been found in THF and $CHCl_3$ solutions. *n*-C_6H_{14} solutions produce a blue-shifted and narrower band. The band shrinkage in alkane solutions has been attributed to the existence of stiff and well-defined dimers,[9] whereas more dynamic 1:1 H_2O−8HQ aggregates in $CHCl_3$ are thought to produce a broader band. The analogue THF solution band appears similar to the $CHCl_3$ one in peak wavelength and width. Et_2O solutions seems particularly similar to *n*-C_6H_{14} solutions in terms of peak wavelength and (more important) bandwidth. This finding could suggest the presence of 8HQ dimers in such a solvent. The CCl_4 solution

band seems somewhat intermediate between $CHCl_3$ solutions and *n*-C_6H_{14} solutions. The presence of a relatively large bandwidth could suggest the existence of H_2O−8HQ adducts similarly to $CHCl_3$ and THF solutions or, at least, less tight dimers in comparison to *n*-C_6H_{14} solutions.

8HQ in Alkane Solution: Assignment of the UV−Vis Spectral Features. According to the experimental work of Bardez et al.,[9] 8HQ in a solution of *n*-heptane principally exists as dimer, at least in the concentration range from 4.7×10^{-3} to 9.4×10^{-3} M, with a dimer stability constant equal to 7×10^7 M^{-1}. This high thermodynamic stability of 8HQ dimers can explain the lack of significant trends in the absorption features observed in a range of concentration from 9×10^{-7} to 2×10^{-3} M in *n*-heptane and cyclohexane. An 8HQ crystal has been reported that can be considered an aggregate of dimers.[31] In this crystal, the 8HQ hydrophilic groups (OH group and the N atom) are responsible for the bond between the two monomers (hydrogen bond), and hydrophobic contacts ($\pi-\pi$ contacts) take place among the dimers. This dimeric structure is possibly preserved in alkane solution and this fact could explain the large solubility of the 8HQ in these apolar solvents. Other hydroxyquinolines (like 7-hydroxyquinoline) are much less soluble in alkane.[9] More interestingly, the 8HQ fluorescence quantum yield in alkane solvents appears very low (2×10^{-4}) if compared to 5-hydoxyquinoline in isopentane (0.30) and 8-methoxyquinoline in isopentane (0.05).[6] In *n*-C_6H_{14} solutions, we have not recorded any significant emission. As discussed in the Introduction, a possible explanation is the occurrence of a fast double proton transfer from the OH groups to N atoms which takes place in the first excited state.[5,9,10] It is not possible at present to establish if this transfer is intramolecular of intermolecular, that is, if it implies or not an exchange of protons between the monomers although the intermolecular channel appears the easiest. Investigations in this sense are in progress in our laboratories by the means of computational approaches. However, the proton-transfer product is considered to be the 8HQ ketonic form, which is supposed to be barely emissive. Because the emission quenching in alkane solutions is evident also at 77 K,[6] the excited-state reaction seems to be associated to a very low (or nonexistent) energy barrier.

We have modeled the 8HQ dimer by the means of *ab-initio* DFT computations. Geometry optimizations at the B3LYP/6-31G(d) level of approximation were performed without use of symmetry constrains and led to structure of C_2 point symmetry. The B3LYP/6-311G(2d,p) level of approximation has been applied to refine the found structure and for the analytical computation of its Hessian. Figure 3 shows that the obtained structure is not planar, differently from the results of the semiempirical computations of Bardez et al.[9] The C_2 rotation axis interchanges the two 8HQ moieties. These geometrical features are also present in 8HQ crystals,[31] where each dimer shows C_2 point group symmetry and its characteristics are similar to the computed ones. Table S2 (in the Supporting Information) lists some computed and experimental geometrical parameters. Both the computations and the experimental values agree in describing the intermolecular hydrogen bond shorter than the intramolecular counterpart; furthermore, the hydrogen bond angle (O−H−N angle) is more favorable to the intermolecular hydrogen bond than the intramolecular one. This fact suggests that the intermolecular ESPT could be favored over the intramolecular one, although we have to remember that this process can only be effective in the excited state of the molecule and, in such a case, the geometry could be different. Furthermore, in each monomer, the hydrogen atom of the OH group is

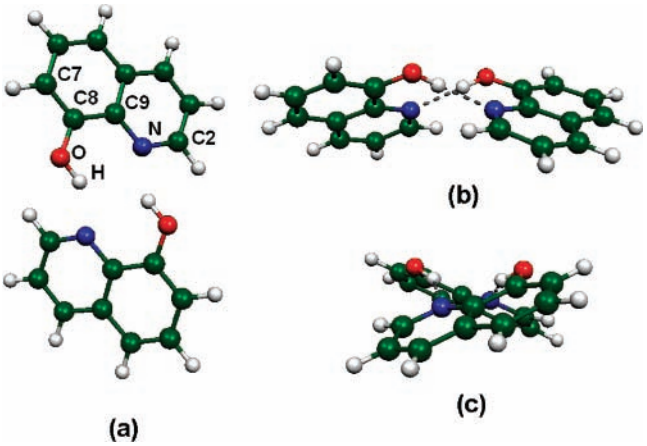

Figure 3. Different views of the computed dimeric form of 8HQ. Some atoms are labeled for reference in Table S2 (in the Supporting Information).

significantly outside the average plane of the remaining atoms by virtue of the torsion around the C−O bond (H−O-C8−C7 parameter in Table S2). In this way, it points more directly toward the nitrogen atom of the nearest molecule and forms a stronger intermolecular hydrogen bond. The sign of the torsion deformation is the same in both computations and X-ray results. Furthermore, their values are similar, especially if we consider that the dimer geometry in the crystal can be influenced by packing effects. For comparison, other dihedral angles associated with the C−O bond are reported and they show the substantial planarity of the remaining part of the monomer.

Table 2 reports the computed energetic and thermodynamic parameters for the dimerization process:

$$8HQ + 8HQ = (8HQ)_2$$

These computations have been performed by treating the molecules in a vacuum. In this situation, the loss of entropy due to the aggregation counterbalances the energetic and enthalpic gains due to the intermolecular hydrogen bonds. Our conclusion is that in the gas phase there is no significant dimerization. Nevertheless, in alkane solutions, the entropy change could be more favorable to dimerization. From the reported value of the dimerization equilibrium constant in *n*-heptane of 7×10^7 M^{-1} at 40 °C,[9] we have a measure of the Gibbs standard energy of −10.7 kcal/mol. A comparison with the computed dimerization standard Gibbs energy (+4.5 kcal/mol at 25 °C, Table 2) and the computed standard enthalpy (−6.7 kcal/mol) at 25 °C, Table 2) clearly indicates that a positive dimerization entropy is the primary cause of dimerization in solution. A similar behavior has been reported for 7-hydroxyquinoline in benzene.[32,33] Furthermore, several examples of the importance of the solvation entropy in dimerization processes are reported in literature.[34,35]

With the aim to verify the effect of the dimerization on the absorption spectrum and to assign the absorption bands of 8HQ, we have performed TD-DFT computations. Figure 4 reports the Kohn−Sham's orbitals energy levels close to the HOMO and LUMO for the monomer and dimer. The energy values are listed in Table S3 (in the Supporting Information). In Figure 5, surface plots of some of the Kohn−Sham's orbitals of the *cis*-8HQ monomer have been reported. The monomer orbitals are labeled according to their symmetry; furthermore, a progressive number has been indicated in parentheses.

It is possible to correlate the energy levels and the Kohn−Sham orbitals of the monomer with a couple of closed-spaced

TABLE 2: Computed Dipole Moment, Electronic Energies, and Thermodynamic Parameters of the *cis*-8HQ Dimer Formation[a]

ΔE_{el} [b] (kcal mol^{-1})	ΔE_{ZP} [c] (kcal mol^{-1})	ΔH^0 (kcal mol^{-1})	ΔS^0 (cal K^{-1} mol^{-1})	ΔG^0 (kcal mol^{-1})	dipole moment (debye)
−7.8	−7.3	−6.7	−37.7	+4.5	2.72

[a] The reported values are associated with the adduct formation from two isolated *cis*-8HQ molecules in their relaxed geometry to the dimeric structure in its relaxed geometry. The collected parameters can be directly referred to the dimerization equilibrium in a vacuum. All the data have been computed at the B3LYP/6-311G(2d,p) level of approximation. The dimer dipole moment lies along the C_2 axis of the molecule and it is perpendicular to the average plane of the dimer structure. For comparison, the dipole moment of the isolated *cis*-8HQ is 2.47 debye at the same level of approximation, and it lies on the plane of the *cis*-8HQ molecular structure. [b] Electronic energy (self-consistent field energy in the Born-Oppeneimer approximation). [c] Electronic energy corrected by the zero-point energies.

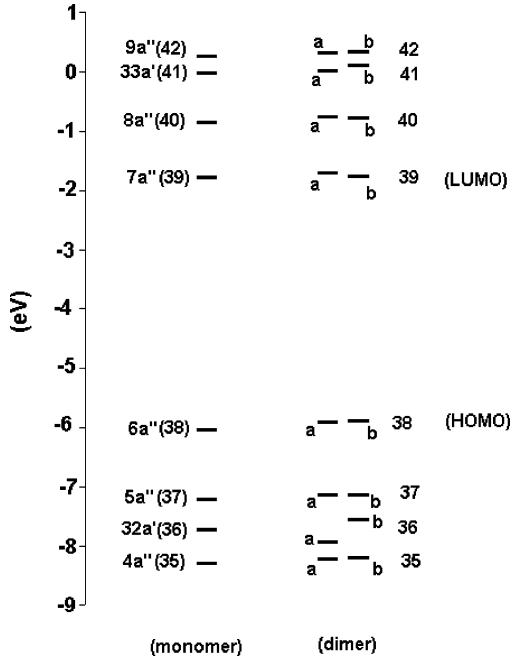

Figure 4. Energy levels of the Kohn−Sham orbitals computed for isolated 8HQ and its dimeric form.

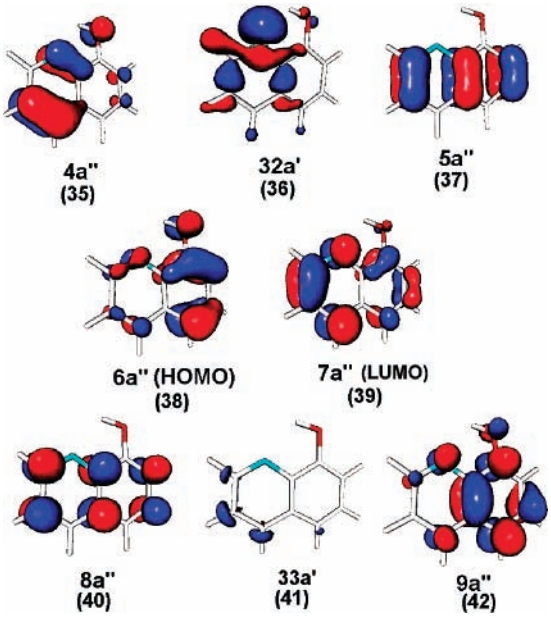

Figure 5. Some 8HQ Kohn−Sham orbitals close in energy to the HOMO and LUMO.

orbitalic energy levels and of the dimer. Each couple can be considered as produced by the in-phase (A symmetry) and out-of-phase (B symmetry) linear combinations of the monomer fragment orbitals (qualitatively reported in Figure 5). Thus, each couple of orbitals has been labeled according to the same progressive number that identifies the monomer orbital. The energy splitting of the two orbitals in each couple is relatively low, apart from orbital 36; it is a σ-type orbital mostly located on the nitrogen atom and pointing outside one monomer. Thus, it is more affected by the presence of the other monomer because it is particularly involved in the intermolecular hydrogen bond. All the other orbitals are π-type orbitals or they point outside the dimer structure, as in the case of the σ-type orbital 33a′ (41); thus they are less influenced by the interactions between the two monomers.

In Table 3, we compare the computed electronic transitions of the monomer and the dimer. The numeric label of the Kohn−Sham orbitals has been used for indicating the excited-state composition in both the monomer and dimer. In the case of the dimer, we have reported the excited-state composition without distinguishing the a and b orbitals of the couple.

The computed absorption spectrum is characterized by two main features both in the monomer and in the dimer. In the *cis*-8HQ monomer (Table 3), they are computed at 340 and 232 nm, with the second feature significantly more intense (oscillator strengths of 0.034 and 0.630, respectively). This description is in good agreement with the experimental findings (Table S1 in the Supporting Information and Figure 2).

The first computed absorption band can be considered a HOMO−LUMO transition in the case of the *cis*-8HQ monomer. In the case of the dimer, the HOMO and the LUMO are almost degenerate with the HOMO−1 and LUMO+1 orbitals, respectively, producing four close-spaced electronic transitions. Among them, the first one at 351 nm is computed as the most intense feature, and it has to be associated with the first absorption at 340 nm in the case of the *cis*-8HQ monomer. The sum of the oscillator strengths of the first four absorptions of the dimer is significantly more than twice the oscillator strength of the monomer (0.103 versus 2×0.034). In our experimental spectra in *n*-C_6H_{14}, we have found that the Lambert−Beer law is satisfied in the concentration range from 10^{-3} to 10^{-7} M. Such a finding could be due to the large dimerization constant of 8HQ in this environment, which prevents the observation of monomeric 8HQ also at the lower concentrations; this fact is in good agreement with the previously discussed 8HQ dimerization constant measured in *n*-heptane.[9] We should note, however, that we observed a substantial invariance of the first experimental band molar absorbivity in different solvents (Table S1). This suggests that, unlike the computational results, the first absorption band of 8HQ is scarcely affected by intermolecular interactions deriving from solvation and/or dimerization.

If we assume that only dimeric 8HQ was the absorbing species in our experimental spectra, an error of +33 nm (−0.37 eV) is to be assigned to the computation of first band peak wavelength. Among the solution spectra, *n*-C_6H_{14} solutions are the most reliable benchmark for our computations because we

TABLE 3: Results of TD-DFT Computations at the B3LYP/6-311+G(2d,p) Level of Approximation Performed on the B3LYP/6-311G(2d,p)-Optimized Geometries[a]

monomer				dimer			
state	λ (nm)	f[b]	composition		λ (nm)	f[b]	composition
^{1}A′	340	0.034	38−39, 87% 38−42, 2%	^{1}B	351	0.090	38−39, 89%
				^{1}A	349	0.006	38−39, 88%
				^{1}A	339	0.001	38−39, 98%
				^{1}B	339	0.006	38−39, 98%
^{1}A′	288	0.004	37−39, 38% 38−40, 61%	^{1}A	291	0.001	37−39, 36% 38−40, 63%
				^{1}B	291	0.010	37−39, 37% 38−40, 62%
				^{1}B	268	0.002	38−40, 100%
				^{1}A	268	0.000	38−40, 100%
^{1}A″	264	0.002	36−39, 95%	^{1}B	264	0.002	36−39, 94%
				^{1}A	261	0.002	36−39, 93%
				^{1}A	253	0.001	37−39, 98%
				^{1}B	253	0.004	37−39, 99%
^{1}A″	232	0.001	38−41, 94% 38−43, 3% 38−44, 2%	^{1}B	236	0.021	38−41, 91% 38−43, 2%
				^{1}A	235	0.003	38−41, 89% 38−43 2%
^{1}A′	232	0.630	35−40, 8% 37−39, 44% 38−40, 25% 37−42, 3%	^{1}A	237	0.115	35−40, 6% 37−39, 46% 38−40, 22% 38−41, 3%
				^{1}B	233	0.971	35−40, 8% 37−39, 41% 38−40, 21% 38−41, 2% 38−42, 3%

[a] Excitation wavelengths, oscillator strengths, and composition of the excited states are reported. Regarding the excited-state composition, the interested Kohn−Sham orbitals are labeled according to Figure 4. In the case of the *cis*-8HQ dimers, the excited-state composition is referred to the couple of almost-degenerate orbitals of Figure 4. [b] Oscillator strength.

have a clear knowledge of the form of 8HQ in such a solvent. However, as discussed in the following, the same information is not guaranteed in other solvents.

The correspondence between the monomer and dimer bands is kept also for the second intense absorption, which is computed at 232 nm for the monomer. It can be associated to the two absorptions at 237 and 233 nm in the case of the dimer; the absorption at 233 nm is more intense, so that the computed peak wavelength can be assigned to its value. In this case, the sum of the oscillator strengths of the two dimer bands is less than twice the oscillator strength of the monomer transition (1.086 vs 2×0.630). These computed features are easily assigned to the second experimental band (Table S1); also in this case, we have found that the Lambert−Beer law is followed in the concentration range from 10^{-4} to 10^{-7} M. However, differently from the first absorption band, the second band appears more affected by solvation in terms of molar absorbivity and shape. The fact that the spectrum does not vary also at the lowest concentration indicates that 8HQ is mainly dimeric also at 10^{-7} M. Because the experimental band is placed at 243 nm in *n*-C_6H_{14}, we can evaluate an inaccuracy of −10 nm (+0.12 eV) versus the computed value.

Other low-intensity features have been computed between the two principal features. The monomer shows two absorptions at 288 and 264 nm. The dimer counterparts are the four absorptions between 291 and 261 nm with a maximum at 291 nm. Also in this case, the monomer−dimer correspondence is clear. All these transitions are predicted as relatively weak bands; thus, it is not surprising that no features have been observed between the two main bands in the experimental spectra.

8HQ in Chlorinated Solvents: H_2O−8HQ Adducts. According to vapor pressure osmometry measurements,[9] 8HQ in chlorinated solvents principally exists as an adduct with one H_2O molecule in the concentration range from 1.03×10^{-2} to 5.14×10^{-2} M. It has been supposed that competition between the internal hydrogen bond and the hydrogen bond with the H_2O molecule allows a significant fraction of molecules in *trans* conformation, or at least partially breaks the internal hydrogen bond.[6,9] In this situation the ESPT could be much slower and/or the partial disruption of the fluorescence-quenching intramolecular hydrogen bond might lead to a higher emission quantum yield. As a consequence, in chlorinated solvents (and other solvents like THF) 8HQ produces higher quantum yields.[6]

Several 1:1 H_2O−8HQ adducts can be postulated for both *cis*-8HQ and *trans*-8HQ. We have performed geometry optimization with the aim to verify the most likely form of such adducts. Figure 6 shows different adduct structures optimized at the B3LYP/6-311G(2d,p) level of approximation. The *cis*-8HQ and *trans*-8HQ structures are the two isolated 8HQ isomers, with no direct bonds with H_2O molecules. The structures labeled as *cis*-adduct-1, *cis*-adduct-2, and *cis*-adduct-3 have one H_2O molecule bound to *cis*-8HQ, whereas the *trans*-adduct-1 and *trans*-adduct-2 labels are used for the two optimized structures of *trans*-8HQ. Table 4 collects some computed values relative to the structures above; in all the structures, the first excited state reported in Table 4 is the same HOMO−LUMO transition ($\pi-\pi^*$) that we have described in the case of *cis*-8HQ and its dimer. Also the main characteristics of the HOMO and LUMO appear unchanged; thus, Figure 5 can be still considered for a visual characterization of the HOMO and LUMO. The same considerations can be extended to the second absorption band.

Table 4 shows that the *cis*-8HQ isomer is more stable than *trans*-8HQ. Our geometry optimization in the cases of H_2O−

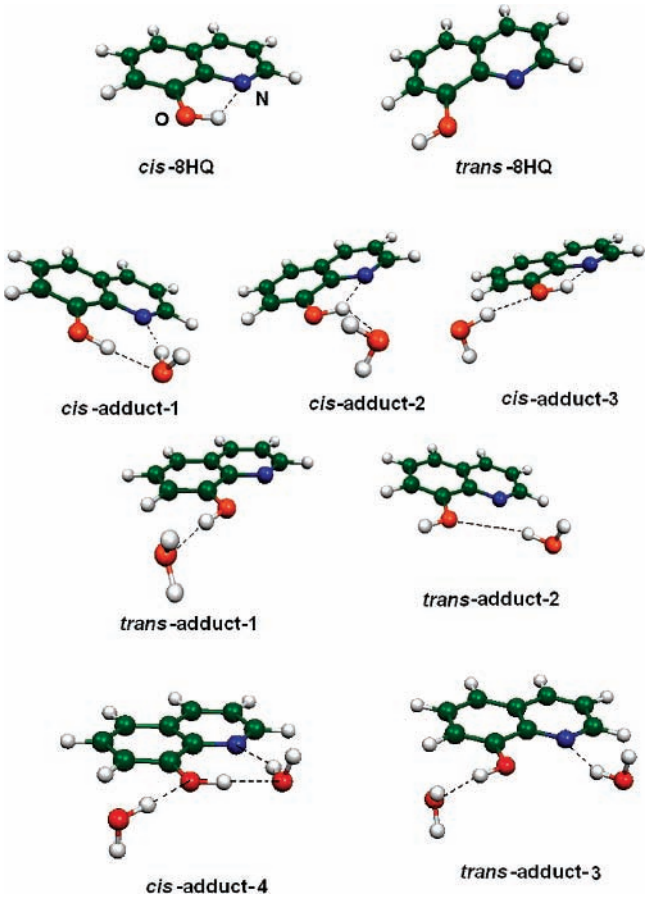

Figure 6. Optimized structures of the 1:1 adducts between H_2O and 8HQ.

8HQ adducts has been achieved by starting from different possible initial geometries, without symmetry constraints, and using large basis sets. The presence of direct interactions between 8HQ and H_2O does not seem to effectively reduce the stability of the two 8HQ conformers. The energy difference between the most stable *cis*-adduct (*cis*-adduct-1) and the most stable *trans*-adduct (*trans*-adduct-1) is 8.8 kcal/mol in a vacuum (DFT computations), to be compared to the 8.3 kcal/mol between isolated *cis*−8HQ and *trans*−8HQ. A second point to be underlined is the higher stability of *cis*-adduct-1 in the class of 1:1 H_2O−8HQ adducts. This is the structure already described by computations in literature;[11] it is characterized by a H_2O molecule interposed between the OH group and N atom.

The presence of two H_2O molecules (*cis*-adduct-4 and *trans*-adduct-3 in Figure 6) seems to reduce the relative stability of *cis*-8HQ and *trans*-8HQ in a vacuum (6.6 kcal/mol from DFT computations). However, the inclusion of solvation in our computations is more effective in this respect. As reported in Table 4, $CHCl_3$ solvation, as treated by the IEF-PCM model, reduces the energy gap between *cis*-8HQ and *trans*-8HQ to about 50% of its value in a vacuum. This is also true for 1:1 H_2O−8HQ adducts. In the case of 2:1 H_2O−8HQ adducts, the energy gap is lowered to 2.6 kcal/mol in $CHCl_3$; the existence of higher aggregates between H_2O an 8HQ has been postulated by Bardez et al.[9] in chlorinated solvents at low 8HQ concentration, but it has not been experimentally demostrated. Here we can say that the increase in the number of H_2O molecules around 8HQ seems to reduce the energy preference for the *cis*-8HQ conformer. At the low concentration used for fluorescence spectra, the 2:1 or superior H_2O−8HQ adducts could allow the existence of a significant fraction of *trans*-8HQ, with possible increased emission quantum yield. However, the preference for the *cis*-8HQ seems to remain quite high so that, in the absorption spectra, it is not possible to observe the small fraction of *trans*-8HQ also at low concentration. Indeed, we have found that the Lambert−Beer law is satisfied in the concentration range from 10^{-4} to 10^{-7} in $CHCl_3$ solutions. Furthermore, as shown in Table 4, the presence of one or two H_2O molecules around 8HQ does not lead to definite changes in the absorption features.

If we assume that in $CHCl_3$ solution the principal form of 8HQ is 1:1 H_2O−8HQ adducts, the *cis*-adduct-1 seems to be the most likely form of 8HQ. Research aimed at studying the excited-state proton transfer of 8HQ should take into account this point, because the H_2O molecule in such a position can take part in the proton transfer through a concerted process. Further computational work in our laboratories quantifies the influence of the H_2O molecule on the kinetics and dynamics of the ESPT.

OH Stretching Frequency. IR spectroscopy can be a valuable tool for confirming the 8HQ conformation in solution. Computations based on the Hartree−Fock theory were accurate in predicting the low-frequency vibrational modes in 1:2 7-hydroxyquinoline−H_2O aggregates;[36] DFT computations at the B3LYP/6-31G(d,p) level of approximation were reliable for the assignment of the 7-hydroxyquinoline OH stretching mode in adducts with methanol.[37]

Not scaled OH stretching in 8HQ dimer were computed at 3383 and 3385 cm^{-1}. The experimental stretching in *n*-C_6H_{14} and cyclohexane have been reported at 3419−3421 cm^{-1},[9] in good agreement with our measure in *n*-C_6H_{14} (3423 nm, Table 1); interestingly, a value of 3420 cm^{-1} has been reported for 8HQ crystals,[38] where 8HQ forms dimeric units as in alkane solutions. Because we have experimental evidence that the form of 8HQ in *n*-C_6H_{14} and cyclohexane is a dimer of *cis*-8HQ,[9] we can think that the computational model is able to predict the stretching frequency with good confidence. In chlorinated solvents, the OH stretching peak has been found at 3411 cm^{-1} in $CHCl_3$ and 3416 cm^{-1} in CCl_4. According to our computation, the *cis*-adduct-1 structure (the most stable H_2O−8HQ adduct in Table 4 and Figure 6) shows two normal modes at 3331 and 3460 cm^{-1} that are a combination of the OH stretching of 8HQ and OH stretching of H_2O. The normal mode at 3460 cm^{-1} is computed to be more intense (more than a factor 10); thus the experimental band can be assigned to the normal mode at 3460 cm^{-1}. All the other 1:1 H_2O−8HQ adducts computed structures show more different OH stretching frequencies (Table 4); in particular this is true for all the *trans*-8HQ structures. Also in this case, the computations suggest that *cis*-8HQ is the preferred form of 8HQ in chlorinated solvents; in particular, *cis*-adduct-1 seems the preferred form. It is noteworthy that *cis*-adduct-4 (the most stable 2:1 H_2O−8HQ adduct) also presents two features that can be assigned to the 8HQ OH stretching; the peak at 3426 cm^{-1} is clearly more intense and in very good agreement to the experimental value in $CHCl_3$ solutions.

Now we can evaluate the effect of adduct formation on the OH stretching frequency. From Table 4, according to the computations, the OH stretching frequency is red-shifted of at least 174 cm^{-1} passing from isolated *cis*-8HQ to *cis*-adduct-1 (the most likely form of 1:1 H_2O−8HQ adducts) and of about 239 cm^{-1} passing from isolated *cis*-8HQ to dimeric 8HQ. It is evident that aggregation has important effects on the OH stretching frequency. In this light, the hypothesis that the 8HQ intramolecular hydrogen bond is the only responsible of the OH stretching frequency invariance in different environments should

TABLE 4: Computed Data of the Optimized Structures Reported in Figure 6 and Dimeric 8HQ (Figure 3)[a]

structure	relative energy DFT (kcal/mol)	relative energy MP2 (kcal/mol)	main absorptions in a vacuum[b] λ (nm)	f	OH stretching in a vacuum (cm^{-1})
dimeric *cis*-8HQ			351 233	0.090 0.971	3383; 3385
cis-8HQ	vacuum: 0.0	vacuum: 0.0	340	0.034	3624
	$CHCl_3$: 0.0	$CHCl_3$: 0.0	232	0.630	
	H_2O: 0.0	H_2O: 0.0			
trans-8HQ	vacuum: +8.3	vacuum: +8.5	317	0.044	3818
	$CHCl_3$: +4.6	$CHCl_3$: +4.6	227	0.651	
	H_2O: +2.5	H_2O: +2.6			
cis-adduct-1	vacuum: 0.0	vacuum: 0.0	358	0.036	3331; 3460
(1:1 H_2O−8HQ)	$CHCl_3$: 0.0	$CHCl_3$: 0.0	236	0.597	
	H_2O: 0.0	H_2O: 0.0			
cis-adduct-2	vacuum: +5.1	vacuum: +4.9	335	0.040	3583
(1:1 H_2O−8HQ)	$CHCl_3$: +4.2	$CHCl_3$: +3.9	231	0.634	
	H_2O: +3.4	H_2O: +3.2			
cis-adduct-3	vacuum: +3.5	vacuum: +4.3	335	0.035	3607
(1:1 H_2O−HQ)	$CHCl_3$: +4.9	$CHCl_3$: +4.2	231	0.638	
	H_2O: +4.5	H_2O: +3.8			
trans-adduct-1	vacuum: +8.8	vacuum: +8.8	317	0.044	3584
(1:1 H_2O−8HQ)	$CHCl_3$: +4.1	$CHCl_3$: +4.2	227	0.651	
	H_2O: +2.1	H_2O: +2.2			
trans-adduct-2	vacuum: +9.9	vacuum: +9.2	320	0.043	3821
(1:1 H_2O−8HQ)	$CHCl_3$: +6.1	$CHCl_3$: +5.4	228	0.654	
	H_2O: +4.1	H_2O: +3.4			
cis-adduct-4	vacuum: 0.0	vacuum: 0.0	348	0.036	3274; 3426
(2:1 H_2O−8HQ)	$CHCl_3$: 0.0	$CHCl_3$: 0.0	230	0.603	
	H_2O: 0.0	H_2O: 0.0			
trans-adduct-3	vacuum: +6.6	vacuum: +6.5	327	0.043	3559
(2:1 H_2O−8HQ)	$CHCl_3$: +2.6	$CHCl_3$: +2.4	226	0.609	
	H_2O: +1.0	H_2O: +0.9			

[a] B3LYP/6-311G(2d,p) level of approximation for energies and OH stretching frequences; B3LYP/6-311+G(2d,p) applied to the B3LYP/6-311G(2d,p) gemetries for the excitation energy and oscillator strength (*f*). MP2/6-311G(2d,p) for MP2 single point computations applied on the DFT geometries. [b] The first and second main absorption bands of 8HQ,.

be rejected. Besides, the similarity in intermolecular interactions influences on the 8HQ OH stretching frequency seems more reasonable.

8HQ in Water. The possibility that solvent molecules disrupt the 8HQ intramolecular hydrogen bond and lead to a higher fraction of *trans*-8HQ should be higher in H_2O solution. From the discussions of the preview paragraphs, the fact that the 8HQ absorption spectrum in H_2O shows the most blue-shifted band at 305 nm is effectively consistent with the presence of a significant fraction of *trans*-8HQ. Goldman and Wehry[6] suggested that such a solvent is the most capable in favoring the *cis*-*trans* isomerization. The very low emission quantum yield in H_2O, even in presence of *trans*-8HQ (which cannot perform an intramolecular ESPT), has been explained as a consequence of the quenching action of the strong H_2O−*trans*-8HQ hydrogen bond[6] and/or the fast intermolecular ESPT between 8HQ and H_2O molecules.[5,9] Both these effects are predicted to be stronger in H_2O than in chlorinated solvents, thus, both of them are possible explanation of the low quantum yield in H_2O.

Because the detection of the OH stretching frequency is impossible in H_2O, we have performed a computation by classic molecular dynamics (MD) simulation of 8HQ solvation in H_2O. Among the results of the simulation, one of the most important points to be evidenced is that a not negligible fraction of the compound can assume the *trans* conformation. Figure 7 shows the population of the 8HQ OH group torsion angle and around the O−C(aromatic) bond rings. From this curve, a 6% population of *trans*-8HQ can be computed; this value is associated to a *cis*-*trans* isomerization equilibrium constant of 16 at 25 °C (K_{eq} = [*cis*-8HQ]/[*trans*-8HQ]) and Gibbs free energy difference of 1.7 kcal/mol. A 6% fraction of *trans*-8HQ inevitably forces to consider the intermolecular ESPT as an effective way to quench emission in H_2O solutions.

The *cis*−*trans* Gibbs energy difference of 1.7 kcal/mol is in good agreement with our *ab-initio* computations which include solvation effects. Table 4 shows that H_2O solvation (even though treated as a polarizable continuum by the IEF-PCM model) neatly changes the relative stability of the *cis*-8HQ and *trans*-8HQ conformers. Passing from vacuum to H_2O solution, the energy difference is reduced from 8.3 to 2.5 kcal/mol for DFT computations and very similar values have been produced by the MP2 computations (Table 4). A still larger change takes place in the case of 1:1 H_2O−8HQ adducts: the energy difference between the most stable *cis*-adduct and the most stable *trans*-adduct passes from 8.8 kcal/mol in a vacuum to 2.1 kcal/mol in H_2O solution (DFT computations). *cis* and *trans* 2:1 H_2O−8HQ adducts (*cis*-adduct-4 and *trans*-adduct-3) show a more similar energy in the presence of H_2O solvation (energy gap of 1.0 kcal/mol). A comparison of the *ab-initio* energies with the MD results leads to the conclusion that in H_2O, like in $CHCl_3$, H_2O−8HQ adducts are the most likely form of 8HQ; however, a doubt remains on the number of H_2O molecules that can be considered actually bound to 8HQ. A crude comparison of the computed energy and MD equilibrium constant should indicate a fraction of 1:1 H_2O−8HQ adducts and a fraction of 2:1 H_2O−8HQ adducts.

MD simulations does not leave doubts about the existence of H_2O−8HQ adducts. Figure 8 shows that the H_2O concentration is much higher (in comparison to bulk concentration) in proximity of 8HQ. Furthermore, the localization of H_2O molecules from the *ab initio* computations is in very good agreement with the description of MD computations. In the case of *cis*-8HQ (Figure 8a), there is a larger concentration of H_2O in the region of the intramolecular 8HQ hydrogen bond; this fact is in good agreement with the higher stability of *cis*-adduct-1 (Figure 6 and Table 4). Accordingly, MD computations describe

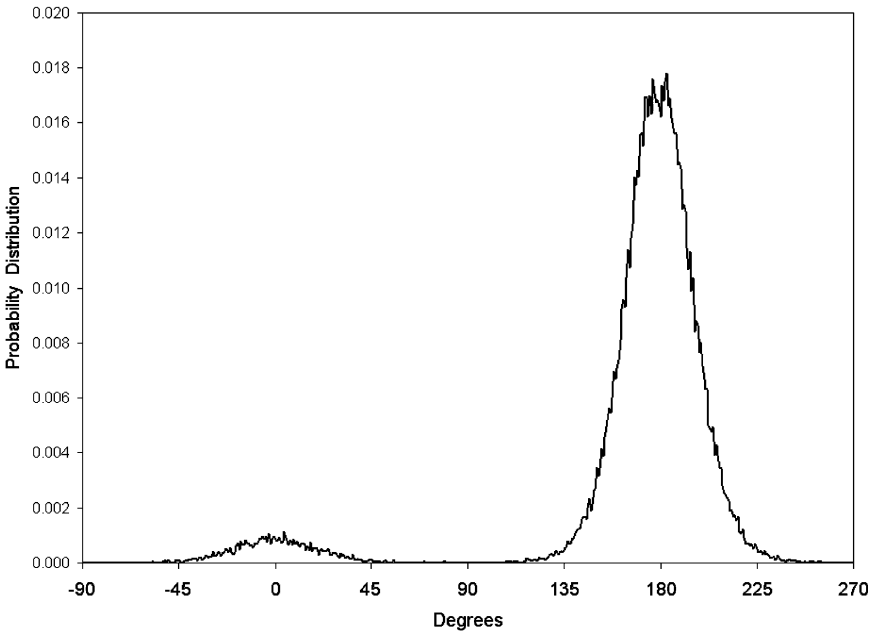

Figure 7. Probability distribution of the torsion angle between the OH group and the aromatic rings of 8HQ. 180° corresponds to a planar *cis*-8HQ; 0° corresponds to a planar *trans*-8HQ. The probability distribution is in arbitrary units.

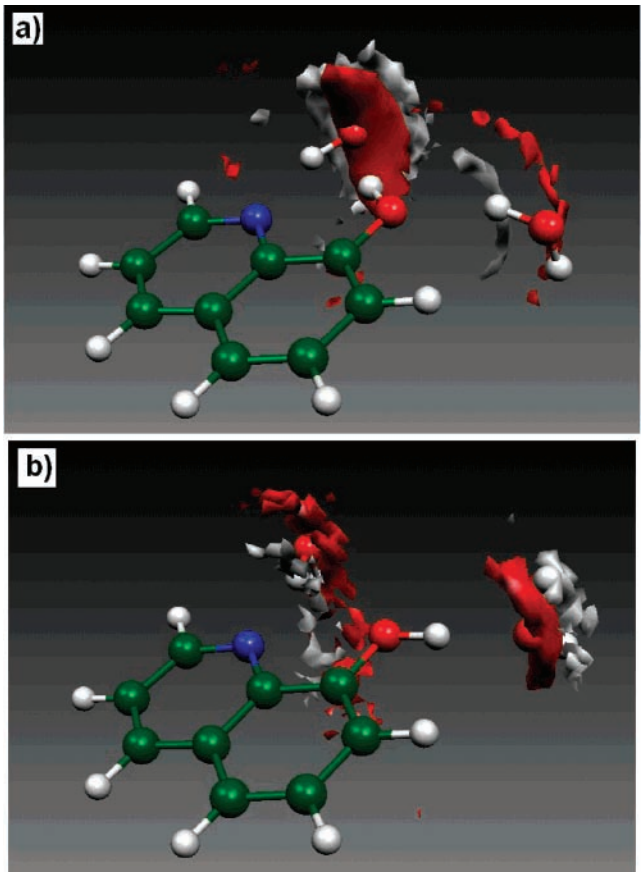

Figure 8. Molecular dynamics results for *cis*-8HQ and *trans*-8HQ in H_2O. The *ab initio cis*-adduct-4 and *trans*-adduct-3 structures (Figure 6) have been included to stress the agreement with the *ab initio* predictions about the H_2O positions. (a) Three-dimensional view of the H_2O oxygen (red) and hydrogen (white) positional probability distribution around *cis*-8HQ. An arbitrary scale from 0 to 10 has been used for the probability distributions. A contour value of 3.3 has been used in the representation. (b) The analogue representation of Figure 8a for *trans*-8HQ; in this case, the used contour value is 2.5 on a scale from 0 to 10.

a smaller probability to find H_2O molecules which form hydrogen bond with the oxygen 8HQ lone pair. In the case of *trans*-8HQ (Figure 8b) a larger concentration of H_2O can be associated to the hydrogen bond between H_2O and the 8HQ OH group (OH acting as acceptor). The nitrogen atom is less capable to bound H_2O molecules, also if a higher (than bulk) concentration of H_2O in its proximity is anyway present. These facts agree with the higher stability of the *trans*-adduct-1 structure from *ab-initio* computations.

From Figure 8 we can expect that 2:1 H_2O-8HQ adducts are not likely in H_2O. In fact, both *cis*-8HQ and *trans*-8HQ show two zones of higher H_2O concentration (the "clouds" in Figure 8), whose relative position is well predicted by *ab initio* computations. However, the probability of finding H_2O molecules in the two zones is very different (the "clouds" have different dimensions). If structures like *cis*-adduct-4 and *trans*-adduct-3 (Figure 6) would be very populated in H_2O, the probabilities to find H_2O in the two zones would be more similar. We can conclude that the existence of such structures cannot be excluded in H_2O, but their population cannot be considered as relevant as the most stable 1:1 H_2O-8HQ adducts (*cis*-adduct-1 and *trans*-adduct-1).

A final note to be discussed regards the shape of the population plot reported in Figure 7 (OH torsion angle) around 180° (the *cis*-8HQ form). A sort of doublet can be seen, with the two peak of the doublet shifted of about +3 and −3° from 180°. We have verified that *ab-initio* computations predict this behavior of the OH torsion angle. In fact, the *cis*-adduct-1 structure shows an OH torsion of 178.5° (−1.5° with respect to 180°). From similar *ab-initio* computations performed on four H_2O molecules around one *cis*-8HQ structure, a torsion angle of about 172° has been detected (the interested reader is directed to the Supporting Information).

Conclusions

8HQ shows a clear preference for the *cis* conformation. This is the most probable form in alkane solutions, where 8HQ is dimeric and seems to preserve the dimeric form found in the crystal structure. Chlorinated solvents are not able to induce a *cis-trans* isomerization also if (at least) one H_2O molecule is

strongly bound to the hydrophilic groups of the molecule. We have verified that, in such a solvent class, even the existence of 2:1 H_2O-8HQ adducts (postulated at low 8HQ concentrations) does not seem sufficient to allow an easy spectroscopically detectable presence of *trans*-8HQ. H_2O solution can be a possible environment for 8HQ isomerization to *trans*-8HQ. Molecular dynamics and *ab-initio* computations agree to predict the presence of a significant fraction of *trans*-8HQ in H_2O.

The presence of *trans*-8HQ in H_2O suggests fluorescence-quenching reaction paths alternate (also if not exclusive) to the intramolecular excited-state proton transfer with a direct participation of solvent cage molecules.

Monomeric 8HQ seems to have a strong affinity toward H_2O molecules in spite of the intramolecular hydrogen bond: H_2O-8HQ aggregates should be always present in H_2O-containing organic solvents apart from alkane solutions (dimeric form) and perhaps Et_2O solutions. In H_2O solutions, 8HQ hydrophilic groups strongly interact with H_2O molecules so to definitely concentrate them in its proximity. As a consequence, 8HQ is normally found as an adduct with H_2O or itself; this explains the similarity in IR OH stretching frequency passing from alkane solutions to more polar organic solutions.

The hypothesis of Goldman and Wehry that the fluorescence quenching in 8HQ is due to the influences of the intramolecular hydrogen bond on the 8HQ OH group is not corroborated by our investigations. The fact that polar organic solvents like $CHCl_3$ and THF allow higher fluorescence quantum yields cannot be associated to the partial disruption of the intramolecular hydrogen bond and consequent stiffer O−H bond. In fact, we know that 8HQ forms a strong hydrogen bond with one H_2O molecule in such solvents. This H_2O molecule is interposed between the OH group and the N atom. Furthermore, the preferred aggregation site of the H_2O molecules is the same observed in water solution where fluorescence is much lower. The small change in OH stretching frequency passing from alkane solutions to $CHCl_3$ and THF solutions should be associated to a similar perturbation induced by the intermolecular interaction rather than the scarce perturbability of the OH group mostly employed in the intramolecular hydrogen bond. Additionally, the OH stretching frequency is lowered (also if by few cm^{-1}) in chlorinated solvents and THF solutions in comparison to alkane solutions, a fact that should be associated to a stronger and stiffer hydrogen bond and lower O−H force constant.

In this light, the ESPT remains the most influential phenomenon to be considered. From the discussions of this paper, such a reaction path can be different in different environments. In alkane solutions, when 8HQ is dimeric, at least a double proton transfer involving the two aggregated 8HQ molecules should be necessary. It seems more probable that the OH protons move from one monomer to the other one, but additional investigations seem necessary for this point. In chlorinated solvents, the H_2O molecule interposed to the 8HQ intramolecular hydrogen bond cannot be omitted (in this respect, ref 11 seems correctly addressed). Its influence on the energetic and characteristics of the tautomerization process appears certain. In water solutions the 1:1 H_2O-cis-8HQ adducts are present in a larger concentration and with a very similar structure in comparison to chlorinated solvents. In this case, the lack of fluorescence also in the presence of a fraction of *trans*−8HQ forces us to consider the direct role of solvent molecules on the proton-transfer paths of both *cis*-8HQ and *trans*−8HQ.

The only hypothesis that we can formulate in this moment is that the ESPT is particularly fast in alkane and H_2O solutions. In the first case, a stiff dimeric structure could favor the proton transfer from one molecule to the other one. In water solutions, the presence of water in the solvation sphere of 8HQ implies very fast H_2O-8HQ and H_2O-H_2O proton exchanges that could quickly lead to the 8HQ ketonic form, also when *trans*-8HQ is involved. In chlorinated solvents or other polar organic solvents, the 1:1 H_2O-cis-8HQ adducts lack the support of H_2O molecules in the solvation cage. In this case, a relatively large part of *cis*-8HQ in the excited state is able to emit light before the quenching tautomerization process is accomplished.

Acknowledgment. This work has been supported by the Italian Ministero dell'Istruzione, dell'Università e della Ricerca (MiUR) through FIRB 2001 (RBNE01P4JF) and from the Centro di Eccellenza CEMIF. CAL (CLAB01TYEF) and PRIN 2005 200503527 grants.

Supporting Information Available: Table of additional information about the UV−vis 8HQ spectra, table of geometrical parameters, table of Kohn−Sham orbital energies, emission spectra of 8HQ, absorbance−concentration plots, additional graphical information about the MD computations in the molecular plane, and the Cartesian coordinates of all the computed structures. This material is available free of charge via the Internet at http://pubs.acs.org

References and Notes

(1) Soroka, K.; Vithanage, R. S.; Phillips, D. A.; Walker, B.; Dasgupta, P. K. *Anal. Chem.* **1987**, *59*, 629.

(2) Hollingshead, R. G. W. *Oxine and Its Derivatives*; Butterworths: London, 1954−1956; Vols. I−IV. Phillips, J. P. *Chem. Rev.* **1955**, *56*, 271. Hollingshead, R. G. W. *Anal. Chim. Acta* **1958**, *19*, 447. Dowlings, S. D.; Seitz, W. R. *Spectrochim. Acta* **1984**, *40A*, 991. Fernandez-Gutierrez, A.; Munoz de la Pena, A. In *Molecular Luminescence Spectroscopy. Methods and Application: Part I*; Schulman, S. G., Ed.; Wiley: New York, 1985; pp 371−546. Farruggia G.; Iotti S.; Prodi L.; Montalti M.; Zaccheroni N.; Savage P. B.; Trapani V.; Sale P.; Wolf F. I. *J. Am. Chem. Soc.* **2006**, *128*, 344.

(3) Isshiki, K.; Tsuji, F.; Kuwamoto, T.; Nakayama, E. *Anal. Chem.* **1987**, *59*, 2491. Firdaus M. L.; Norisuyea K.; Satoa T.; Urushiharaa S.; Nakagawaa Y.; Umetania S.; Sohrina Y. *Anal. Chem. Acta* **2007**, *583*, 296.

(4) Tang, C. W.; VanSlyke, S. A. *Appl. Phys. Lett.* **1987**, *51*, 913. (b) Sheats, J. R.; Antoniadis, H.; Hueschen, M.; Leonard, W.; Miller, J.; Moon, R.; Roitman, D.; Stocking, A. *Science* **1996**, *273*, 884. Amati, M.; Lelj, F. *Chem. Phys. Lett.* **2002**, *358*, 144. Amati, M.; Lelj, F. *Chem. Phys. Lett.* **2002**, *363*, 451. Amati, M.; Lelj, F. *J. Phys. Chem. A* **2003**, *107*, 2560.

(5) Ballard, R. E.; Edwards, J. *J. Chem. Soc.* **1964**, 4868

(6) Goldman, M.; Wehry, E. L. *Anal. Chem.* **1970**, *42*, 1178.

(7) Schulman, S. G. *Anal. Chem.* **1971**, *43*, 285.

(8) Mason, S. F.; Philip, J.; Smith, B. E. *J. Chem. Soc. A* **1968**, 3051. Shulman, S. G.; Gershon, H. *J. Phys. Chem.* **1968**, *72*, 3693.

(9) Bardez, E.; Devol, I.; Larrey, B.; Valeur, B. *J. Phys. Chem. B* **1997**, *101*, 7786.

(10) Cheatum, C. M.; Heckscher, M. M.; Crim, F. F. *Chem. Phys. Lett.* **2001**, *349*, 37.

(11) Li, Q.-S.; Fang, W.-H. *Chem. Phys. Lett.* **2002**, *367*, 637.

(12) Demas, J. N.; Crosby, G. A. *J. Phys. Chem.* **1971**, *75*, 991.

(13) Nakamaru, K. *Bull. Soc. Chem. Jpn.* **1982**, *5*, 2697.

(14) Becke, A. D. *J. Chem. Phys.* **1993**, *98*, 5648.

(15) Szabo, A.; Ostlund, N. S. *Modern Quantum Chemistry*, revised first edition; McGraw-Hill, Inc.: New York, 1989; Chapter 6.

(16) Tomasi, J.; Mennucci, B.; Cammi, R. *Chem. Rev.* **2005**, *105*, 2999.

(17) Casida, M. Time dependent density functional response theory for molecules. In *Recent advances in Density Functional Methods*; Chong, D. P., Ed.; World Scientific: Singapore, 1995; Vol. 1, p 155.

(18) Casida, M. E.; Jamorski, C.; Casida, K. C.; Salahub, D. R. *J. Chem. Phys.* **1998**, *108*, 4439.

(19) Frisch, M. J.; Trucks, G. W.; Schlegel, H. B.; Scuseria, G. E.; Robb, M. A.; Cheeseman, J. R.; Montgomery, J. A., Jr.; Vreven, T.; Kudin, K. N.; Burant, J. C.; Millam, J. M.; Iyengar, S. S.; Tomasi, J.; Barone, V.; Mennucci, B.; Cossi, M.; Scalmani, G.; Rega, N.; Petersson, G. A.; Nakatsuji, H.; Hada, M.; Ehara, M.; Toyota, K.; Fukuda, R.; Hasegawa, J.; Ishida, M.; Nakajima, T.; Honda, Y.; Kitao, O.; Nakai, H.; Klene, M.; Li, X.; Knox, J. E.; Hratchian, H. P.; Cross, J. B.; Adamo, C.; Jaramillo, J.; Gomperts, R.; Stratmann, R. E.; Yazyev, O.; Austin, A. J.; Cammi, R.;

Pomelli, C.; Ochterski, J. W.; Ayala, P. Y.; Morokuma, K.; Voth, G. A.; Salvador, P.; Dannenberg, J. J.; Zakrzewski, V. G.; Dapprich, S.; Daniels, A. D.; Strain, M. C.; Farkas, O.; Malick, D. K.; Rabuck, A. D.; Raghavachari, K.; Foresman, J. B.; Ortiz, J. V.; Cui, Q.; Baboul, A. G.; Clifford, S.; Cioslowski, J.; Stefanov, B. B.; Liu, G.; Liashenko, A.; Piskorz, P.; Komaromi, I.; Martin, R. L.; Fox, D. J.; Keith, T.; Al-Laham, M. A.; Peng, C. Y.; Nanayakkara, A.; Challacombe, M.; Gill, P. M. W.; Johnson, B.; Chen, W.; Wong, M. W.; Gonzalez, C.; Pople, J. A. *Gaussian 03*, revision B.05; Gaussian, Inc.: Pittsburgh, PA, 2003.

(20) Schaftenaar, G.; Noordik, J. H. *J. Comput.-Aided Mol. Design* **2000**, *14*, 123 (www.cmbi.kun.nl/~schaft/molden/molden.html).

(21) *Molekel 4.3*, Fluckiger, P.; Luthi, H.P.; Portmann, S.; Weber, J. Swiss Center for Scientific Computing, Manno (Switzerland), 2000−2002; Portmann, S.; Luthi, H. P. MOLEKEL: An Interactive Molecular Graphic Tool. *CHIMIA* **2000**, *54*, 766.

(22) Case, D. A.; Pearlman, D. A.; Caldwell, J. W.; Cheatham, T. E.; Ross, W. S., III; Simmerling, C. L.; Darden, T. A.; Merz, K. M.; Stanton, R. V.; Cheng, A. L.; Vincent, J. J.; Crowley, M.; Tsui, V.; Radmer, R. J.; Duan, Y.; Pitera, J.; Massova, I.; Seibel, G. L.; Sing, U. C.; Weiner, P. K.; Kollman, P. A. AMBER 6, University of California, San Francisco, 1999. Pearlman, D. A.; Case, D. A.; Caldwell, J. W.; Ross, W. S.; Cheatham, T. E.; DeBolt, S., III.; Ferguson, D.; Seibel, G.; Kollman, P. A. *Comp. Phys. Commun.* **1995**, *91*, 1

(23) Jorgensen, W. L.; Chandrasekhar, J.; Madura, J. D.; Impey, R. W.; Klein, M. L. *J. Chem. Phys.* **1983**, *79*, 926.

(24) Cornell, W. D.; Cieplak, P.; Bayly, C. I.; Gould, I. R.; Merz, K. M., Jr.; Ferguson, D. M.; Spellmeyer, D. C.; Fox, T.; Caldwell, J. W.; Kollman, P. *J. Am. Chem. Soc.* **1995**, *117*, 5179.

(25) Singh, U. C.; Kollman, P. A. *J. Comput. Chem.* **1984**, *5*, 129.

(26) Berendsen, H. J. C. *J. Chem. Phys.* **1984**, *81*, 3684.

(27) Darden, T.; York, D.; Pedersen, L. *J. Chem. Phys.* **1993**, *98*, 10089.

(28) Ryckaert, J. P.; Ciccotti, G.; Berendsen, H. J. C. *J. Comput. Phys.* **1977**, *23*, 327.

(29) Badger, G. M.; Moritz, A. G. *J. Chem. Soc.* **1958**, 3437

(30) Richards, J. H.; Walker, S. *Trans. Faraday Soc.* **1961**, *57*, 406.

(31) Banerjee, T.; Saha, N. N. *Acta Crystallogr., Sect. C* **1986**, *42*, 1408.

(32) Chou, P.-T.; Wei, C.-Y-.; Wang, C.-R. C.; Hung, F.-T.; Chang, C.-P. *J. Phys. Chem. A* **1999**, *103*, 1939.

(33) In the case of ref 32, *ab-initio* computations gives a positive dimerization standard Gibbs energy of +1.82 kcal/mol for the most stable 7-hydroxyquinoline dimer, whereas the experimental standard Gibbs energy in benzene solution has been reported as −4.2 kcal/mol.

(34) Rohatgi, K. K.; Singhal, G. S. *J. Phys. Chem.* **1966**, *70*, 1695. Calderone, C. T.; Williams, D. H. *J. Am. Chem. Soc.* **2000**, *123*, 6262. Leung, M.-K.; Mandal, A. B.; Wang, C.-C.; Lee, G.-H.; Peng, S.-M.; Cheng, H.-L.; Her, G.-R.; Chao, I.; Lu, H.-F.; Sun, Y.-C.; Shiao, M.-Y.; Chou, P.-T. *J. Am. Chem. Soc.* **2001**, *124*, 4287. Baraldi, I.; Caselli, M.; Momicchioli, F.; Ponterini, G.; Vanossi, D. *Chem. Phys.* **2002**, *275*, 149. Kemnitz, K.; Yoshihara, K. *J. Phys. Chem.* **1991**, *95*, 6095.

(35) Kemnitz et al.[34] discussed the importance of entropy in establishing the dimer stability of xanthene dyes in apolar solvents; a positive dimerization entropy is considered the principal responsible of the dimerization process. This class of compounds is characterized by aromatic structures with polar substituents, like 8HQ, and this fact suggests a possible similar explanation of the 8HQ dimerization in alkane solutions.

(36) Bach, A.; Coussan, S.; Müller, A.; Leutwyler, A. *J. Chem. Phys.* **2000**, *112*, 1192.

(37) Matsumoto, Y.; Ebata, T.; Mikami, N. *J. Phys. Chem. A* **2002**, *106*, 5591.

(38) Krishnakumar, V.; Nagalakshmi, R.; Janaki, P. *Spectrochim. Acta Pt. A* **2005**, *61*, 1097.